JPhys Materials

PAPER • OPEN ACCESS

# Magnetotransport as a probe for the interplay between Sm and Fe magnetism in SmFeAsO

To cite this article: M Meinero *et al* 2023 *J. Phys. Mater.* **6** 014005

Journal of Physics: Materials

PAPER

# Magnetotransport as a probe for the interplay between Sm and Fe magnetism in SmFeAsO

M Meinero[1,2,*], F Caglieris[1,2], A Leveratto[2], L Repetto[1], M Fujioka[3], Y Takano[4], U Zeitler[5], I Pallecchi[2] and M Putti[1,2]

[1] Department of Physics, University of Genova, Via Dodecaneso 33, 16146 Genova, Italy
[2] SPIN-CNR, Corso Perrone 24, 16152 Genova, Italy
[3] Research Institute for Electronic Science, Hokkaido University, N20W10, Sapporo, Hokkaido 001-0020, Japan
[4] National Institute for Materials Science (NIMS), Tsukuba, Ibaraki 305-0047, Japan
[5] High Field Magnet Laboratory (HFML-EMFL), Radboud University, Toernooiveld 7, 6525ED Nijmegen, The Netherlands
[*] Author to whom any correspondence should be addressed.

**E-mail:** martina.meinero@spin.cnr.it

**Keywords:** unconventional superconductivity, iron-based superconductors, magnetoresistance, magnetic transitions

Supplementary material for this article is available online

**OPEN ACCESS**

**RECEIVED**
21 July 2022

**REVISED**
10 November 2022

**ACCEPTED FOR PUBLICATION**
29 November 2022

**PUBLISHED**
20 December 2022



## Abstract

The complex magnetic ordering of parent compounds of most unconventional superconductors is crucial for the understanding of high-temperature superconductivity (SC). Within this framework, we have performed temperature-dependent magnetotransport experiments on a single crystal of SmFeAsO, a parent compound of iron pnictide superconductors. We observe multiple features in the measured transport properties at temperatures below the antiferromagnetic (AFM) ordering of Sm, $T < T_{NSm}$, which evolve with in-plane magnetic field, suggesting a rich variety of metamagnetic transitions never before observed in this compound. Considering that transport mainly involves Fe d orbitals at the Fermi level, these findings suggest that the features originate from magnetic transitions of the Fe moments sublattice, which in turn may be induced by magnetic transitions of the Sm moments sublattice via the interaction between Fe and Sm moments. We outline a possible scenario in which the Fe moments, strongly affected by the Sm ordering below $T_{NSm}$, reorder to an in-plane canted AFM structure, which is washed out by the application of an in-plane magnetic field up to 9 T. Our work shows that transport properties are a valuable tool for investigating magnetic ordering in iron pnictide parent compounds, where the interplay of magnetism and SC is believed to be the origin of high-temperature SC.

## 1. Introduction

The interplay between superconductivity (SC) and magnetism has been a hot topic since the discovery of SC. Over the decades, magnetic ordering has passed from being regarded as antagonist to SC to being observed as coexisting with it, and eventually to being identified as responsible for the unconventional mechanism of Cooper pairing. The discovery of SC in iron-based superconductors (IBSs) [1] has boosted research on this topic, as this class of materials offers a unique environment for studying the entanglement between SC and magnetism [2–4].

The REFeAsO (magnetic rare-earth RE = Ce, Pr, Nd and Sm) parent compounds of the so-called 1111 family of IBSs are characterized by multiple antiferromagnetic (AFM) orderings. A tetragonal-to-orthorhombic phase transition is followed by a commensurate AFM ordering of Fe, with the Fe moments directed along the orthorhombic $a$-axis, coupled ferromagnetically along the $b$-axis and antiferromagnetically along the $a$-axis [3]. Generally, SC emerges upon the suppression of long-range AFM order by means of chemical doping or external pressure [5] and the highest critical temperature, $T_c = 58$ K, is reached in the $SmFeAsO_{1-x}F_x$ system [6].

In addition, a spontaneous AFM ordering of the RE moments is observed below $T_{NRE} = 4.4$, 11, 6 and 4.6 K for RE = Ce [7], Pr [8], Nd [9] and Sm [10], respectively. In this regard, it is observed that the lighter RE elements (Ce and Pr) order in-plane [7, 11, 12] whereas the heavier RE elements (Nd and Sm) order along the *c*-axis [9, 13–16].

The interplay between the AFM orderings of Fe and RE moments has been widely discussed, and it has been recently emphasized that the RE magnetism may influence the AFM spin fluctuations of Fe through an interplay between RE and Fe magnetism, resulting in the enhancement of $T_c$ [12, 14].

The effect of RE ordering has been always considered subtle and elusive, although a correlation with the superconducting phase has been proved to some extent. In Ce [7], Pr [17] and Nd [13] systems it has been reported that the AFM ordering of both Fe and RE, occurring in the parent compounds, is suppressed upon doping before the onset of SC. On the contrary, in the $SmFeAsO_{1-x}F_x$ system (which exhibits the highest $T_c$), long-range AFM Sm order and SC coexist over a wide range of compositions [16, 18, 19]. Interestingly, a beneficial effect of long-range AFM order of Sm on SC has been previously observed in other classes of superconductors. In $SmRh_4B_4$ [20] and $Sm_{1.85}Ce_{0.15}CuO_{4-y}$ [21] compounds, the critical magnetic field $H_{c2}$ increases below $T_{NSm}$, indicating a significant correlation between the Sm magnetic moments and the superconducting phase. In particular, for $SmRh_4B_4$ it has been proposed that an alternative superconducting pairing, other than a standard Bardeen–Cooper–Schrieffer pairing state, is more stable under an AFM molecular field [22]. In the $SmFeAsO_{1-x}F_x$ system, the extremely high $H_{c2}$ has prevented a direct experimental exploration of the effect of Sm ordering on the superconducting phase diagram.

Considering that in IBSs the Fe 3d orbitals contribute mainly to the density of states at the Fermi level [23], the electronic (and superconducting) properties are extremely sensitive to any modification in the Fe magnetic ordering. A rearrangement of the Fe moments due to interaction with the RE magnetic order has been observed in REFeAsO (RE = Nd, Ce and Pr) compounds via several experimental techniques including resistivity measurements, neutron and x-ray diffraction, neutron and synchrotron resonant x-ray magnetic scattering, muon spin relaxation measurements and Mössbauer spectroscopy [9, 11, 24–26].

Concerning SmFeAsO, x-ray magnetic scattering performed on single crystals [27] shows that the in-plane as well as the out-of-plane correlations of Fe moments are modified upon the spontaneous ordering of Sm [27]. However, the large thermal neutron absorption cross section for Sm makes neutron diffraction rather challenging with Sm-based materials [15].

Interestingly, the electrical resistivity shows an anomaly in correspondence with $T_{NSm}$ [28–30] as a signature of the interplay between Sm magnetic moments and conduction electrons. However, from *ab initio* calculations it emerges that the 4f orbitals of Sm lie well below the Fermi energy [31], so that they cannot be directly responsible for the change in the electrical transport. More realistically, the charge carriers feel the effect of Sm ordering on Fe moments.

In this work, we thoroughly investigate the temperature dependence of the resistivity as well as the Hall coefficient and the magnetoresistance of a high-quality SmFeAsO single crystal in magnetic fields up to 9 T applied in different directions with respect to the crystallographic axes and the electrical current. We propose magnetotransport as an alternative and sensitive probe of magnetic ordering in REFeAsO compounds and, in particular, of Sm and Fe sublattices below $T_{NSm}$, where experimental data are missing. Indeed, we observe multiple features in our data which reveal that transport is strongly affected by the long-range AFM order of Sm and suggest a strong interaction between Sm and Fe magnetism, with possible implications for the pairing mechanism at the basis of high-temperature SC.

## 2. Methods

### 2.1. Sample preparation

The single crystal of SmFeAsO was prepared by a flux method using CsCl, as described in [32]. The size of the crystal was 9.8 $\mu$m × 5.1 $\mu$m × 0.6 $\mu$m ($a \times b \times c$) and a focused ion beam was used to deposit four W leads to prepare the sample for the four-probe transport measurements, as shown in the scanning electron microscope image in the inset of figure 1(b) and already reported in [33].

### 2.2. Magneto-transport measurements

Electrical resistivity, Hall effect and magnetoresistance measurements were performed in a range of temperature $T$ between 2 and 300 K and by sweeping the magnetic field $B$ from −9 to 9 T using a Quantum Design PPMS. We also performed Hall effect measurements between $T = 0.4$ K and 4.2 K and $B$ up to 30 T using a Bitter-type resistive magnet. We performed all the measurements with both positive and negative $B$ in order to separate the even and odd parts of the signal with respect to the magnetic field. In particular, the Hall effect and the magnetoresistance were respectively obtained by the $B$-odd and $B$-even part of the voltage signal measured in the four-probe configuration (see also Supplementary Data [34] for further details).

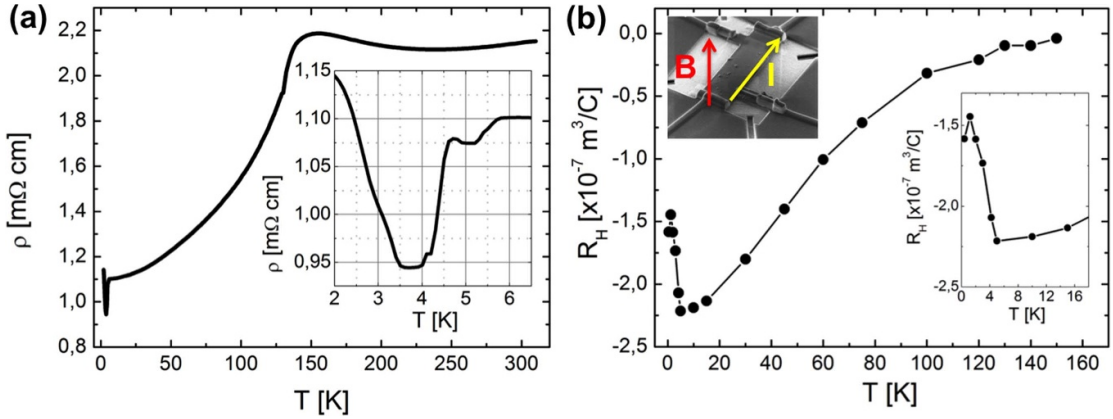


**Figure 1.** (a) Electrical resistivity from 2 to 320 K. Inset: enlarged view of the data between 2 and 8 K. (b) $R_H$ from 0.4 K to 150 K. Top-left inset: SEM images of the crystal with W electrical contacts. Right inset: zoom of the data between 0.4 K and 18 K.

## 3. Results

### 3.1. Electrical resistivity, Hall coefficient and magnetoresistance measurements

Figure 1(a) shows the electrical resistivity $\rho$ of the SmFeAsO crystal as a function of temperature. Two different major features are clearly distinguishable: (a) the structural and magnetic transition associated with the AFM ordering of Fe which occurs at $T_{NFe} = 138$ K determines an abrupt reduction of the curve below $T_{NFe}$ and (b) the AFM ordering of Sm occurring at $T_{NSm} \sim 6$ K is followed by another drop in $\rho$. Notably, the magnification of the low-temperature region reported in the inset of figure 1(a) clearly shows other features that have never been identified before to the best of our knowledge and will be discussed in detail later on in this paper.

Figure 1(b) shows the Hall coefficient $R_H$ extracted from Hall effect measurements between 0.3 and 150 K measured under standard conditions (with $B$ applied parallel to the $c$-axis and the current applied in the $ab$-plane). Below $T_{NFe}$, $R_H$ is negative and increases in absolute value with decreasing $T$ and an abrupt upturn occurs below $T_{NSm}$ (see inset of figure 1(b)), suggesting a reorganization of the electronic bands, as already observed in similar systems [26, 35].

Caglieris *et al* [33] reports magnetoresistance measurements of the same SmFeAsO single crystal when $B$ is applied out-of-plane (parallel to the $c$-axis, perpendicular to the electrical current). To briefly summarize, below $T_{NSm}$, the compound exhibits an extremely high positive (cyclotronic) magnetoresistance which reaches the 300%–400% of the zero-field value $\rho(0)$ for $B = 30$ T in the temperature range 0.4–4.2 K. On the contrary, when $B$ is applied in-plane, the magnetoresistance does not show Shubnikov–de Haas oscillations due to the two-dimensional character of the Fermi surface. At $T = 340$ mK, the magnetoresistance is always negative (reaching −25% around 10 T) with a sharp drop around 5 T and a smooth rise up to 30 T. For $T > T_{NSm}$, the magnetoresistance is small and positive, reaching values between 0.4% and 0.6% at 9 T for $T$ in the range 6–15 K (see figure S2 in the supplemental material of [33]).

We will now consider only the $B$ in-plane configuration since it is not affected by the cyclotronic contribution and it is therefore more favorable for observing the evolution of the anomalies present in $\rho$ below $T_{NSm}$.

Both the configurations with $B$ parallel and $B$ perpendicular to the current are tested, giving virtually identical results. This comparison suggests that no appreciable role is played by the orientation of the applied current with respect to the magnetic field. In the following, the data with $B$ perpendicular to the current are reported, whereas the data with $B$ parallel to the current are reported in the Supplementary Data [34]. On the other hand, it is not possible to investigate whether there is any difference between configurations of field aligned along either the $a$ or the $b$ planar orthorhombic axes, due to domain twinning.

Figure 2 shows the temperature dependence of $\rho$ in the range 2–10 K at selected $B$ values between 0 T and 9 T. We first notice that an intriguing dependence of $\rho$ on $B$ is observed at selected temperatures below $T_{NSm}$, whereas no significant $B$ dependence was measured above this. Furthermore, from figure 2(a) it appears that the resistivity drop related to the Sm ordering is completely suppressed when $B = 9$ T.

The magnetoresistance, defined as $\rho(B) - \rho(0)/\rho(0)$, is shown in figure 2(b). All the curves saturate to a positive value at $B_{sat}$. $B_{sat}$ decreases with increasing $T$, and this corresponds to the suppression of resistivity drop shown in figure 2(a). Below $B_{sat}$ all the magnetoresistance curves decrease with decreasing $B$ (figure 2(b)) and exhibit peculiar features that shift to higher fields as $T$ decreases. Furthermore, it can be

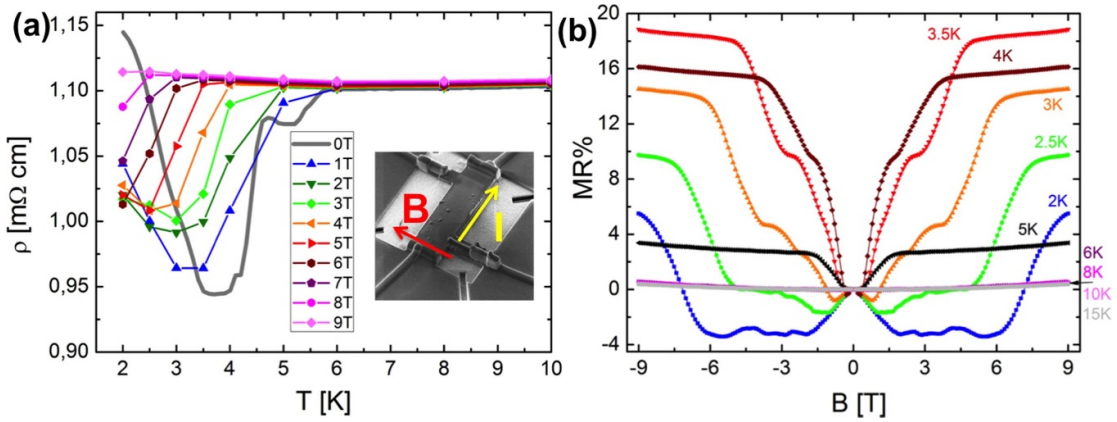


**Figure 2.** (a) Temperature dependence of the electrical resistivity between 2 and 10 K at selected magnetic fields $B$ between 0 and 9 T applied perpendicular to the electrical current $I$, as shown in the inset. (b) $B$-dependence of the magnetoresistance from −9 T to 9 T at selected temperatures in the range 2–15 K.

noted that at low field and low temperature, the magnetoresistance shows a significant negative contribution, which is progressively suppressed with increasing temperature and field, disappearing above 3.5 K. We may conclude that this negative contribution is related to the upturn of $\rho$, which occurs below 3.5 K (see figure 2(a)).

### 3.2. Evolution with $B$ and $T$ of the detected features at $T < T_{NSm}$

We have shown above that below $T_{NSm}$ the electrical resistivity of SmFeAsO as a function of both $T$ (figure 1(a)) and $B$ (figure 2(b)) is characterized by many features, which we now analyze in detail.

Figure 3(a) shows $\rho$ versus log($T$) from 2 to 7 K, where we mark with symbols all the features we detected. Starting from a first saturation level ($\rho \sim 1.10$ mΩ cm), $\rho$ exhibits a first drop (dark cyan 'X') at 6 K, which identifies $T_{NSm}$. At around 4.7 K, $\rho$ shows another jump anticipated by a tiny upturn (feature '#2'). At 4.1 K, feature '#1' indicates a small step-like feature.

Below 4 K, $\rho$ reaches a second saturation level around 0.94 mΩ cm and it starts increasing below 3.5 K (violet crosses), where an additional contribution dominates. Interestingly, $\rho$ increases logarithmically with decreasing $T$ down to 2.3 K, where it starts to saturate again, approaching 1.15 mΩ cm at 2 K. Taking into account the two-dimensional character of the electronic structure of SmFeAsO (see, e.g., in [33]), it is reasonable to assume that the logarithmic temperature dependence of $\rho$ is due to weak localization (WL) [36].

From figure 2(b) it can be noted that the initial decrease of the magnetoresistance for $T < 3.5$ K, which is suppressed at relatively low $B$ values (∼2 T at 2 K), is likely to be due to WL. Indeed, the experimental data can be fitted with the Hikami–Larkin–Nagaoka equation [37], yelding phase coherence lengths from 25 nm at 2 K to 12 nm at 3 K (see Supplementary data [34]).

Figure 3(b) shows $\rho(B)$ up to 9 T applied in plane (see inset of figure 2(a)) for selected temperatures in the range 2–5 K. The curves are rigidly shifted by offsets proportional to $T$ in order to catch by eye the linear temperature shift of the features already discussed in figure 3(a).

Figure 3(c) is a phase diagram where it is possible to follow the evolution with $B$ of the features we observed in $\rho(T)$ when $B = 0$ T (figure 3(a)). Starting from $T_{NSm}$ (dark cyan cross in figures 3(a) and (c)), it is clear that the drop detected in $\rho(T)$ is related to the $B$ values at which $\rho(B)$ curves saturate (black 'X' symbols in figure 3(b)) and in figure 3(c) we call these values '$B_{sat}$'. In particular, with increasing $T$, $B_{sat}$ decreases almost linearly with a slope around $-2.4$ T K$^{-1}$ so that at 2 K a field of $B_{sat} = 9$ T is enough to suppress the drop of $\rho(T)$ which occurs at $T_{NSm}$ (as already noted in figure 2(a)). On the other hand, Riggs *et al* [16] showed that $T_{NSm}$ is almost unchanged by the applied $B$ up to 35 T (in figure 3(c) the dark cyan diamonds represent their data up to 16 T).

Feature '#2' (green empty squares) and feature '#1' (dark yellow empty circles) can be tracked in all the curves below 5 K and 4 K, respectively. They both shift to higher $B$ with decreasing $T$ with a slope around $-2$ T K$^{-1}$.

The WL contribution (violet crosses) is reduced by the applied $B$ with a slope of $-1.2$ T K$^{-1}$.

Interestingly, this plethora of features survives when $B$ is rotated by 90° in the $ab$-plane, parallel to the direction along which the current is applied (see Supplementary Data [34]). This suggests that the physical

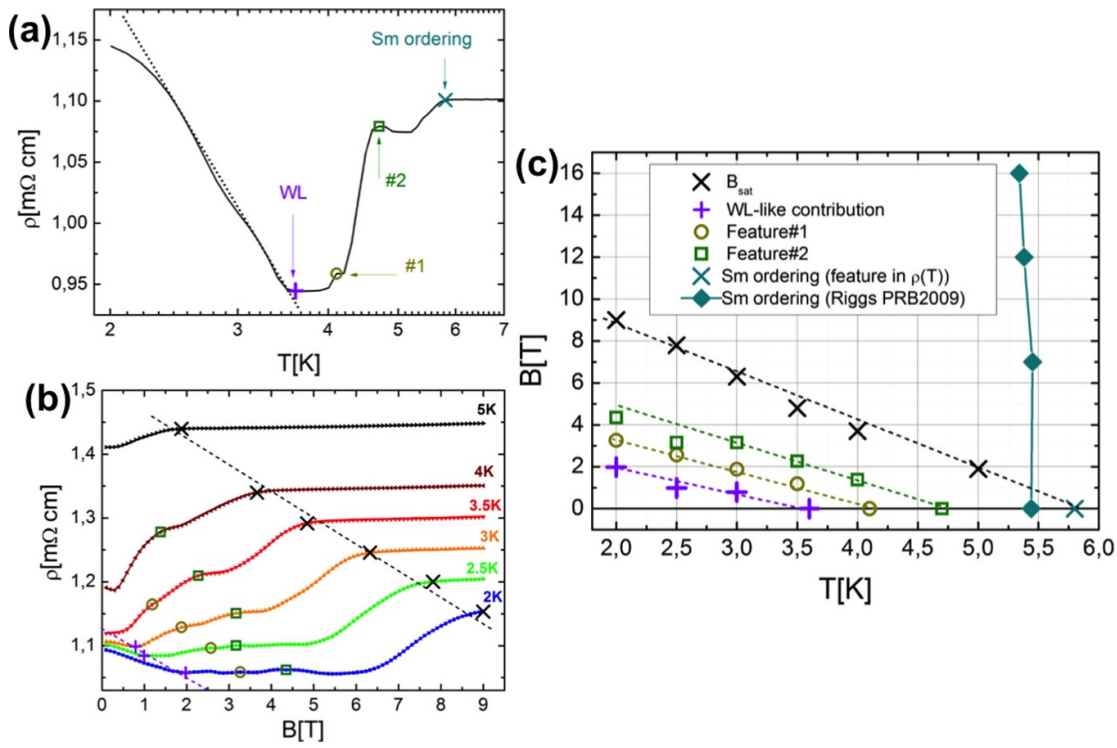


**Figure 3.** (a) Electrical resistivity versus log($T$) between 2 and 7 K. $T_{NSm}$ is marked by the cyan 'X' symbol, an empty green square and an empty dark yellow circle mark the features '#2' and '#1', respectively. The onset of the weak localization (WL) contribution is indicated by a violet cross and the dashed line is a guide to the eye to show the logarithmic increase of $\rho$ due to the WL contribution. (b) $\rho(B)$ curves up to 9 T at selected temperatures in the range 2–5 K. The curves are shifted to avoid overlaps. The violet crosses mark the onset of the WL contribution, the dark yellow circles and green squares mark the features and the black 'X' symbols mark $B_{sat}$. (c) Evolution with temperature and magnetic field of the features shown in (a) and (b).

mechanism at play does not substantially depend on the specific orientation of $B$ in the *ab*-plane and with respect to the current.

## 4. Discussion

Although this unusual magnetoresistive phenomenology is evidently triggered by Sm spin ordering at $T_{NSm}$, it is improbable that the observed features are directly related to some $B$-induced metamagnetic transitions of the Sm magnetic moments.

In fact, it has been observed that $T_{NSm}$ is almost insensitive to applied $B$ up to 35–40 T, where a metamagnetic anomaly in the Sm AFM ordering has been observed [16, 38] and successfully predicted by Yang *et al* [39].

Hence, causing a canting of the Sm moments probably requires much higher fields than those used in our experiments. In addition, as the Sm ordering is out-of-plane it is expected to be less sensitive to the action of $B$ in-plane. On the other hand, transport properties of the SmFeAsO parent compound must be sensitive to the magnetic ordering of Fe moments. Indeed, the orientation of the Fe d orbitals is distorted by the magnetic arrangement of Fe moments, as a consequence of the spin–orbit interaction. As transport properties are dominated by Fe d orbitals crossing the Fermi level, the orientation of Fe magnetic moments certainly affects the electronic band structure at the Fermi level, and possibly also affects the scattering probability in Fe d orbitals. Consequently, we believe that the transitions observed in magnetoresistance are related to rearrangements of the Fe magnetic sublattice.

In analogy with what was observed in (Eu,Ca)$Fe_2As$ [40], NdFeAsO [9], CeFeAsO [11] and PrFeAsO [24–26], where a rearrangement of the Fe ordering is observed in correspondence to the RE ordering, we propose that below $T_{NSm}$, Fe moments order to a different magnetic structure, as already suggested by both Nandi *et al* [27] and Maeter *et al* [24]. With lowering $T$, approaching $T_{NSm}$, the magnetic interaction between Sm and Fe moments is enhanced. In this way, the charge carriers, strongly dependent on the Fe ordering, are indirectly influenced by the Sm transition, which plays the role of a trigger for Fe magnetic rearrangement. In particular, Maeter *et al* [24] considered the action of the RE magnetic order on the Fe subsystem in REFeAsO (RE = La, Ce, Pr and Sm) and proposed different types of canted Fe structures that are induced by different

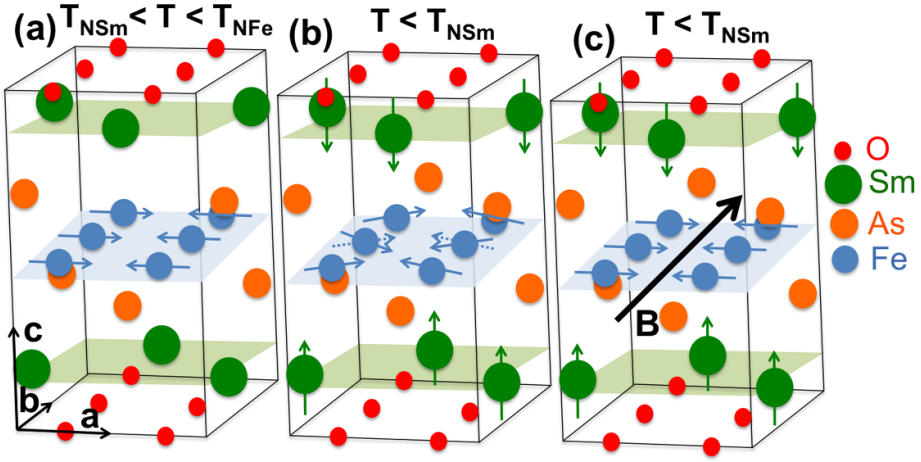


**Figure 4.** (a) Magnetic structure of SmFeAsO for $\mathbf{T_{NSm} < T < T_{NFe}}$ The Fe moments are directed along the orthorhombic *a*-axis, coupled ferromagnetically along the *b*-axis and antiferromagnetically along the *a*-axis. (b) For $T < T_{NFe}$, the Sm moments order ferromagnetically and *ab* planes ordered antiferromagnetically along the *c*-axis, with the Sm moments parallel to the *c*-axis. Noncollinear (solid arrows) and collinear (dashed arrows) in-plane canted Fe structures are induced by the out-of-plane Sm ordering. (c) The AFM Fe structure is progressively restored by the application of an in-plane magnetic field *B*.

RE magnetic structures. For an out-of-plane RE order (as in the case of Sm), they find two possible Fe magnetic orderings, namely AFM collinear and noncollinear in-plane structures (figure 4(b)). In our sample, the resistivity anomalies for 4 K $< T <$ 5.6 K are probable evidence of this transition.

Remarkably, a large enough in-plane magnetic field ($B_{sat} = 9$ T at 2 K), applied either parallel or perpendicular to the current, is able to exactly restore the resistivity value measured just above $T_{NSm}$. This strongly suggests that the in-plane *B* progressively forces the system back to the pristine magnetic order, through successive transitions that at $B = B_{sat}$ eventually restore the AFM alignment of Fe moments existing above $T_{NSm}$, as shown in figure 4. We believe that this *B*-induced transition cannot be a complete spin–flop transition, whose final configuration consists of all the Fe spins aligned ferromagnetically along *B*. In fact, according to Yang *et al* [39] this should happen for $B = 164$ T.

To summarize this discussion, we sketch the proposed phases to which the transitions observed in figure 3 can be tracked down: figure 4 reports the pristine AFM configurations (a), the most plausible canted AFM configurations predicted by Maeter *et al* [24] (b) and the AFM pristine configuration that is restored by the applied magnetic field (c).

We suggest that the features detected in the electrical resistivity below $T_{NSm}$ are due to the rearrangement of Fe moments owing to their interaction with Sm moments. Moreover, we suggest that the features in the magnetoresistance indicate critical field values at which the Fe moments progressively flip to restore the pristine AFM configuration.

Both a theoretical study and other (more detailed) spectroscopic and magnetic measurements performed below $T_{NSm}$ would help to shed light on the coupling between Sm and Fe moments in the SmFeAsO system, with possible consequences for SC, which is still an open issue.

Since Sm ordering survives the onset of SC in many $SmFeAsO_{1-x}F_x$ compounds [16, 18, 19], these intriguing issues could be studied through in-plane and out-of-plane $H_{c2}$ measurements down to low *T* to test the effects of Sm ordering on the superconducting state. This information is lacking due to the very high $H_{c2}$ of $SmFeAsO_{1-x}F_x$ compounds, which does not allow for a direct measurement down to low *T*. However, $T_c$, and accordingly $H_{c2}$, can be progressively suppressed in $SmFeAsO_{1-x}F_x$ compounds by partial substitution of Fe with d elements (Ru, Mn, Ni) [41, 42] without affecting the Sm ordering [35]. Another possibility is to investigate Co-doped SmFeAsO compounds, which show maximum $T_c$s of tens of K [43–45]. These compounds with moderate $T_c$ can give experimental access to the full superconducting phase diagram and could shed light on the effects of Sm ordering on the superconducting state.

## 5. Conclusion

In summary, by means of magnetotransport property measurements, we have investigated the interplay between Sm and Fe sublattices below $T_{NSm}$ in the SmFeAsO system. In particular, the electrical resistivity shows multiple anomalies below $T_{NSm}$, which correspond to magnetic transitions of the Fe moments occurring in zero field. An in-plane field, $B_{sat} = 9$ T at 2 K, either perpendicular or parallel to the electric

current, is able to remove all the resistivity anomalies. For $B < B_{sat}$, the magnetoresistance below $T_{NSm}$ is characterized by many features, which track the evolution with $B$ of the anomalies measured in the electric resistivity. In analogy with other REFeAsO systems (RE = Ce, Nd, Pr), and as already proposed for SmFeAsO, our data strongly support the scenario that below $T_{NSm}$ the Fe moments order to an in-plane canted AFM configuration and the pristine AFM configuration is completely restored by $B_{sat} = 9$ T at 2 K. We also suggest that the features detected in the magnetoresistance below $B_{sat}$ are due to the progressive restoration of the pristine AFM configuration of the Fe moments. Our data clearly show that the Sm AFM ordering strongly affects the charge carriers through the interaction with the magnetic sublattice of Fe, and this interaction could play a role in the pairing mechanism at the basis of high-temperature SC, as already reported for other Sm-based systems.

## Data availability statement

The data that support the findings of this study are available upon reasonable request from the authors.

## Acknowledgments

We thank Da-Yong Liu and Liang-Jian Zou for the fruitful discussions.

The authors acknowledge funding from the Italian Ministry of Education, University and Research (MIUR) through the 'Dipartimenti di Eccellenza' project 2018-2022 and support by the Italian MIUR projects: PRIN 'HiBiSCUS' grant no. 201785KWLE. Part of this work was supported by HFML-RU/NWO-I, member of the European Magnetic Field Laboratory (EMFL).

## ORCID iDs

M Meinero https://orcid.org/0000-0003-2729-5825
F Caglieris https://orcid.org/0000-0002-9054-580X
A Leveratto https://orcid.org/0000-0001-8480-2884
M Fujioka https://orcid.org/0000-0002-5829-6591
I Pallecchi https://orcid.org/0000-0001-6819-6124

## References

[1] Kamihara Y, Watanabe T, Hirano M and Hosono H 2008 *J. Am. Chem. Soc.* **130** 3296
[2] Johnston D C 2010 *Adv. Phys.* **59** 803
[3] Lumsden M D and Christianson A D 2010 *J. Phys.: Condens. Matter* **22** 203203
[4] Dai P 2015 *Rev. Mod. Phys.* **87** 855
[5] Paglione J and Greene R 2010 *Nat. Phys.* **6** 645–58
[6] Fujioka M *et al* 2013 *Supercond. Sci. Technol.* **26** 085023
[7] Zhao J *et al* 2008 *Nat. Mater.* **7** 953–9
[8] Kimber S A J *et al* 2008 *Phys. Rev.* B **78** 140503(R)
[9] Tian W *et al* 2010 *Phys. Rev.* B **82** 060514(R)
[10] Tropeano M, Martinelli A, Palenzona A, Bellingeri E, Galleani d'Agliano E, Nguyen T D, Affronte M and Putti M 2008 *Phys. Rev.* B **78** 094518
[11] Zhang Q *et al* 2013 *Phys. Rev.* B **88** 174517
[12] Kim M G, Ratcliff W, Pajerowski D M, Kim J-W, Yan J-Q, Lynn J W, Goldman A I and Kreyssig A 2021 *Phys. Rev.* B **103** 174405
[13] Qiu Y *et al* 2008 *Phys. Rev. Lett.* **101** 257002
[14] Kim M G, Kim J-W, Yan J-Q, Goldman A I and Kreyssig A 2019 *Phys. Rev.* B **100** 224401
[15] Ryan D H, Cadogan J M, Ritter C, Canepa F, Palenzona A and Putti M 2009 *Phys. Rev.* B **80** 220503
[16] Riggs S, Tarantini C, Jaroszynski J, Gurevich A, Palenzona A, Putti M, Nguyen T D and Affronte M 2009 *Phys. Rev.* B **80** 214404
[17] Zhao J *et al* 2008 *Phys. Rev.* B **78** 132504
[18] Ding L, He C, Dong J K, Wu T, Liu R H, Chen X H and Li S Y 2008 *Phys. Rev.* B **77** 180510(R)
[19] Drew A J *et al* 2008 *Phys. Rev. Lett.* **101** 097010
[20] Hamaker H C, Woolf L D, MacKay H B, Fisk Z and Maple M B 1979 *Solid State Commun.* **31** 139
[21] Dalichaouch Y, Lee B W, Seaman C L, Markert J T and Maple M B 1990 *Phys. Rev. Lett.* **64** 599
[22] Machida K, Nokura K and Matsubara T 1980 *Phys. Rev. Lett.* **44** 821
[23] Singh D J and Du M-H 2008 *Phys. Rev. Lett.* **100** 237003
[24] Maeter H *et al* 2009 *Phys. Rev.* B **80** 094524
[25] McGuire M A, Hermann R P, Sefat A S, Sales B C, Jin R, Mandrus D, Grandjean F and Long G J 2009 *New J. Phys.* **11** 025011
[26] Bhoi D, Mandal P, Choudhury P, Pandya S and Ganesan V 2011 *J. Appl. Phys.* **110** 113722
[27] Nandi S *et al* 2011 *Phys. Rev.* B **84** 054419
[28] Martinelli A *et al* 2008 *Supercond. Sci. Technol.* **21** 095017
[29] Cimberle M R, Canepa F, Ferretti M, Martinelli A, Palenzona A, Siri A S, Tarantini C, Tropeano M and Ferdeghini C 2009 *J. Magn. Magn. Mater.* **321** 3024–30
[30] McGuire M A, May A F and Sales B C 2012 *J. Solid State Chem.* **191** 71–75
[31] Bernardini F *et al* 2019 *J. Phys.: Condens. Matter* **31** 244001

[32] Fujioka M, Denholme S J, Tanaka M, Takeya H, Yamaguchi T and Takano Y 2014 *Appl. Phys. Lett.* **105** 102602
[33] Caglieris F, Leveratto A, Pallecchi I, Bernardini F, Fujioka M, Takano Y, Repetto L, Jost A, Zeitler U and Putti M 2017 *Phys. Rev.* B **96** 104508
[34] See supplemental material for: Hall resistivity measurements and magnetoresistance measurements when B is applied parallel to I
[35] Meinero M *et al* 2021 *Sci. Rep.* **11** 14373
[36] Abrahams E, Anderson P W, Licciardello D C and Ramakrishnan T V 1979 *Phys. Rev. Lett.* **42** 673–6
[37] Hikami S, Larkin A I and Nagaoka Y 1980 *Prog. Theor. Phys.* **63** 707–10
[38] Weyeneth S *et al* 2011 *Phys. Rev.* B **83** 134503
[39] Yang L-L, Liu D-Y, Chen D-M and Zou L-J 2016 *Chin. Phys.* B **25** 027401
[40] Jin W T, Meven M, Sazonov A P, Demirdis S, Su Y, Xiao Y, Bukowski Z, Nandi S and Brückel T 2019 *Phys. Rev.* B **99** 140402(R)
[41] Sanna S, Carretta P, Bonfà P, Prando G, Allodi G, De Renzi R, Shiroka T, Lamura G, Martinelli A and Putti M 2011 *Phys. Rev. Lett.* **107** 227003
[42] Singh S J, Shimoyama J, Yamamoto A, Ogino H and Kishio K 2013 *Physica* C **494** 57–61
[43] Qi Y, Gao Z, Wang L, Wang D, Zhang X and Ma Y,2008 *Supercond. Sci. Technol.* **21** 115016
[44] Wang C *et al* 2009 *Phys. Rev.* B **79** 054521
[45] Qi Y-P, Wang L, Gao Z-S, Wang D-L, Zhang X-P, Zhang Z-Y and Ma Y-W. 2010 *EPL* **89** 67007